# Enhanced Vibration Controllability by Minor Structural Modifications

Raphael T. Haftka,* Zoran N. Martinovic,† and William L. Hallauer Jr.‡
*Virginia Polytechnic Institute and State University, Blacksburg, Virginia*

**A procedure for checking whether small changes in a structure have the potential for significant enhancements of its vibration control system is described. The first step in the procedure consists of the calculation of the sensitivity of the required strength of the control system to small changes in structural parameters. The second step consists of the optimization of the structural parameters to produce maximal reduction in required control system strength with minimal change in the structure. The procedure has been demonstrated for a flexible beam supported by four cables and controlled by a rate feedback, single-colocated, force-actuator velocity-sensor pair. Large changes in control strength requirement were obtained with small structural modifications. Analytical predictions of such effects have also been validated experimentally.**

## Nomenclature

$[C]$ = damping matrix $(n \times n)$
$C_f$ = actuator force per unit current
$C_v$ = sensor voltage per unit velocity
$c$ = viscous damping coefficient, control strength
$e(t)$ = excitation signal
$F$ = force generated by control system, defined in Eq. (23)
$G$ = control gain
$g_b$ = constraints on the damping ratios or real parts of eigenvalues defined in Eqs. (21) and (22)
$g_{hj}$ = $j$th constraint on the magnitude of change of the design variable
$h_i$ = thickness of the $i$th beam element
$i$ = structural design variable number, or electrical current
$j$ = $(-1)^{1/2}$
$K$ = power amplifier transduction constant
$[K]$ = stiffness matrix $(n \times n)$
$[K^*]$ = $(2n \times 2n)$ matrix defined in Eq. (5)
$\ell$ = number of controlled modes
$L$ = subscript denoting a lower limit on $r$th eigenpair damping ratio
$[M]$ = mass matrix $(n \times n)$
$[M^*]$ = $(2n \times 2n)$ matrix defined in Eq. (4)
$m_i$ = $i$th lumped mass
$n$ = number of system degrees of freedom
$r$ = mode number
$\{q(t)\}$ = state vector $(2n \times 1)$
$\{q_0\}_r$ = $r$th eigenvector $(2n \times 1)$
$U$ = subscript denoting upper limit on real part of $r$th eigenvalue
$\{u\}$ = displacement vector $(n \times 1)$
$t$ = time
$\{x\}$ = structural design parameter vector
$\{y\}$ = design variable vector $\{y\} = \{c,x\}$
$\zeta_r$ = damping ratio of $r$th eigenvalue defined in Eq. (10)
$\lambda_r$ = $r$th pair of eigenvalues defined in Eq. (8)
$\sigma_r$ = real part of $r$th eigenvalue defined in Eq. (8)
$\tau$ = time constant defined in Eq. (18)
$\omega_r$ = imaginary part of $r$th eigenvalue defined in Eq. (8)
$\omega_{0r}$ = $r$th frequency defined in Eq. (10)

Received March 21, 1984; revision received Oct. 4, 1984. This paper is declared a work of the U.S. Government and therefore is in the public domain.

*Professor, Department of Aerospace and Ocean Engineering. Member AIAA.
†Graduate Research Assistant, Department of Aerospace and Ocean Engineering. Member AIAA.
‡Associate Professor, Department of Aerospace and Ocean Engineering. Member AIAA.

## Introduction

LARGE space structures will face difficult problems of vibration control. Because of the requirement for low weight, such structures will probably lack the stiffness and damping required for adequate passive control of vibrations. Therefore, a great deal of work is currently in progress on designing active vibration control systems for such structures (see Ref. 1 for some recent work).

Most active control studies assume that the structural configuration is determined from other considerations and that the control system has to be designed for a specified structure. The design effort is typically focused on the control law as well as the number and location of actuators (e.g., Refs. 2-4). Recently, however, there has been some interest in simultaneous design of the structure and the control system so as to produce a truly optimum configuration (e.g., Ref. 5). Reference 5 assumes that simultaneous design is unquestionably a good approach. But the results of such an integrated design approach do not always justify the effort and expense involved (e.g., Ref. 6). Therefore, before embarking on such an ambitious undertaking, it is important to determine if, and under what circumstances, there is a synergistic effect in designing a structure and its control system simultaneously. The purpose of the present paper is to investigate the possibility of such a synergistic effect.

The method used to assess the potential synergistic effect is determination of whether small structural modifications can produce large reductions in the control strength required to achieve a desired level of active damping. If this is indeed the case, then the synergistic effect is established and there is justification to attempt simultaneous structure-control system design of large space structures.

Two methods are proposed for assessing the potential of small structural modifications for reducing significantly the control requirements. The first method is the calculation of the sensitivity of the control requirements with respect to structural parameters. The second is the optimization of structural parameters toward the goal of reducing control requirements, subject to a constraint limiting variations in the structural parameters to small values.

The two methods are demonstrated for a flexible beam supported by four cables and controlled by a rate feedback, single-colocated force-actuator velocity-sensor pair. Small changes in the structure consist of adding small masses and making small changes in the thickness. The synergistic potential is predicted from a finite element model of the system and then validated by a laboratory experiment.

## Calculation of Eigenvalues and Their Derivatives

The structure-control system equation of motion for a structure with $n$ degrees of freedom (DOF) and rate feedback control produced by velocity sensors and actuators is

$$[M]\{\ddot{u}\}+[C]\{\dot{u}\}+[K]\{u\}=\{0\} \tag{1}$$

For a single colocated sensor-actuator pair, the damping matrix $[C]$ has only one nonzero entry, equal to $c$, at the diagonal position corresponding to the controlled DOF.

In state vector form, Eq. (1) becomes

$$[M^*]\{\dot{q}\}+[K^*]\{q\}=\{0\} \tag{2}$$

where

$$\{q\}^T=[\{\dot{u}\}^T\{u\}^T] \tag{3}$$

is the state vector $(2n\times 1)$, and

$$[M^*]=\begin{bmatrix}[0] & [M]\\ [M] & [C]\end{bmatrix} \tag{4}$$

$$[K^*]=\begin{bmatrix}-[M] & [0]\\ [0] & [K]\end{bmatrix} \tag{5}$$

Assuming a solution of Eq. (2) of the form

$$\{q(t)\}=e^{\lambda t}\{q_0\} \tag{6}$$

the associated eigenvalue problem becomes

$$(\lambda[M^*]+[K^*])\{q_0\}=\{0\} \tag{7}$$

The solution of Eq. (7) yields $n$ complex conjugate eigenvalue pairs,

$$\lambda_r=\sigma_r\pm j\omega_r, \qquad r=1,2,\ldots,n \tag{8}$$

The damping factor of the $r$th mode is

$$\zeta_r=-\sigma_r/(\sigma_r^2+\omega_r^2)^{1/2} \tag{9}$$

The real and imaginary parts of $\lambda_r$ may be written in terms of a nominal frequency $\omega_{0r}$ and $\zeta_r$ as

$$\sigma_r=-\zeta_r\omega_{0r}, \qquad \omega_r=\omega_{0r}(1-\zeta_r^2)^{1/2} \tag{10}$$

For the design of the structure and control system, we require the derivatives of the eigenvalues $\lambda_r$ with respect to design parameters $x_i$. These derivatives may be calculated by finite differences, but this can become quite expensive. Therefore, analytical derivatives have been derived (in a manner similar to that of Ref. 7) and employed.

Differentiating Eq. (7) with respect to a design variable $x_i$ for the $r$th eigenpair, one obtains

$$(\lambda_r[M^*]+[K^*])\frac{\partial\{q_0\}_r}{\partial x_i}+\frac{\partial\lambda_r}{\partial x_i}[M^*]\{q_0\}_r + \left(\lambda_r\frac{\partial[M^*]}{\partial x_i}+\frac{\partial[K^*]}{\partial x_i}\right)\{q_0\}_r=\{0\} \tag{11}$$

After premultiplying Eq. (11) by the transpose of the $r$th eigenvector and rearranging terms, one obtains

$$\frac{\partial\lambda_r}{\partial x_i}=\frac{-\{q_0\}_r^T(\lambda_r\partial[M^*]/\partial x_i+\partial[K^*]/\partial x_i)\{q_0\}_r}{\{q_0\}_r^T[M^*]\{q_0\}_r} \tag{12}$$

Equation (12) can also be expressed in the following form,

$$\frac{\partial\lambda_r}{\partial x_i}=\frac{\partial\sigma_r}{\partial x_i}\pm j\frac{\partial\omega_r}{\partial x_i} \tag{13}$$

The derivative of the damping ratio for the $r$th mode is obtained by differentiating Eq. (9) with respect to the design variable $x_i$,

$$\frac{\partial\zeta_r}{\partial x_i}=\frac{\omega_r(\sigma_r\partial\omega_r/\partial x_i-\omega_r\partial\sigma_r/\partial x_i)}{(\sigma_r^2+\omega_r^2)^{3/2}} \tag{14}$$

The derivatives of $\zeta_r$ can be used to assess the potential of small structural modifications for reducing the control requirement. This control requirement is measured by the amount of damping, $c$, supplied by the colocated velocity sensor and actuator. Assume, for example, that we require a minimum level of $\zeta_r$

$$\zeta_r\geq\zeta_{Lr}, \qquad r=1,2,\ldots,\ell \tag{15}$$

where $\zeta_{Lr}$ is the specified minimum. Assume first that this requirement is critical only for one mode, say, the fifth. That is, when we apply the minimal amount of $c$ that would satisfy Eq. (15), then $\zeta_5=\zeta_{L5}$, but $\zeta_r>\zeta_{Lr}$ for $r$ not equal to 5. The effect of small changes in the structural design variables on the required $c$ would then be completely determined by the derivatives of $\zeta_5$ because for small changes in the structure it would remain the only critical mode. Consider, for example, the effect of a change in design variable $x_i$ on $c$. It is determined from the condition that

$$d\zeta_5=\left(\frac{\partial\zeta_5}{\partial c}\right)dc+\left(\frac{\partial\zeta_5}{\partial x_i}\right)dx_i \tag{16}$$

is equal to zero so that $\zeta_5$ remains at $\zeta_{L5}$. Therefore

$$\frac{dc}{dx_i}=-\frac{(\partial\zeta_5/\partial x_i)}{(\partial\zeta_5/\partial c)} \tag{17}$$

If the requirement of Eq. (15) is critical for several modes, then Eq. (17) has to be evaluated for each critical mode, and the lowest value of $dc/dx_i$ represents the actual possible gain.

## Design Method

An initial structure is selected first, and a simple control system is designed for it. The control system design has to satisfy some prescribed minimum levels of active damping. To accomplish this, one increases $c$ until all $\zeta_r$ meet or exceed their specified minimum levels. This is classical control system design based on a specified structure.

Next, a set of structural design variables is selected, and an optimization procedure is employed to calculate the values of the structural variables that minimize the control strength required. Changes in the structural variables are constrained to a small percentage of their values for the initial structure, and the same prescribed minimum levels of active damping are imposed on control system design as before. This is simultaneous structure-control system design.

The synergistic effect is considered to be established if the relative reduction in the control strength required is much larger than the relative changes in structural variables.

Two quantities are used here as measures of modal control effectiveness or level of damping in the system. One is the damping factor $\zeta_r$, and the other is the real part of eigenvalue $\sigma_r$, as defined in Eq. (8). Note that the real part of an eigenvalue $\sigma$ is related to the time $\tau$ required for the amplitude of vibration to be reduced by the factor of $1/e$ as

$$\tau = -1/\sigma \tag{18}$$

## Optimization Procedure

The selection of the structural parameter vector $\{x\}$ was accomplished by defining the design variable vector $\{y\} = \{c,x\}$ and solving the following minimization problem: Minimize $c$, such that

$$g_b(y) \geq 0, \qquad r = 1,2,\ldots,\ell \tag{19}$$

and

$$g_{hj}(x) \geq 0 \tag{20}$$

where $g_b(y)$ represents a lower limit on the damping ratio $\zeta_r$ of the form,

$$g_b = \zeta_r - \zeta_{Lr} \tag{21}$$

or an upper limit on the real part

$$g_b = \sigma_{Ur} - \sigma_r \tag{22}$$

and $g_{hj}(x)$ represents constraints on the magnitude of change of the design variables.

The NEWSUMT optimization program[8] has been used to solve the optimization problem. NEWSUMT employs an extended interior penalty function formulation using Newton's method with approximate second derivatives for each unconstrained minimization.

## Finite Element Model

The theory developed above has been applied for several numerical cases based on an existing small laboratory structure, which consists of a vertical beam and cables in tension suspending the beam (Fig. 1). The structure is represented by a uniform steel beam 2.03 m long with rectangular cross section (51 mm wide × 3.2 mm thick). The beam is attached to floor and ceiling by four 2.3-mm diam steel cables as shown on Fig. 1. Beam finite elements of equal length with displacements and rotations as structural DOFs are used to model the beam. A string-in-tension finite element represents each cable. The model includes geometric stiffness matrices accounting for tension in beam elements. The tension used at the top of the beam is 362 N, and it is proportionally reduced down the beam by the effect of gravity. Small lumped masses representing control system coils and cable clamps are added to the model.

Inherent passive structural damping is not included in the analysis because it is small in comparison with the active damping imposed by the controller. Active damping is ef-

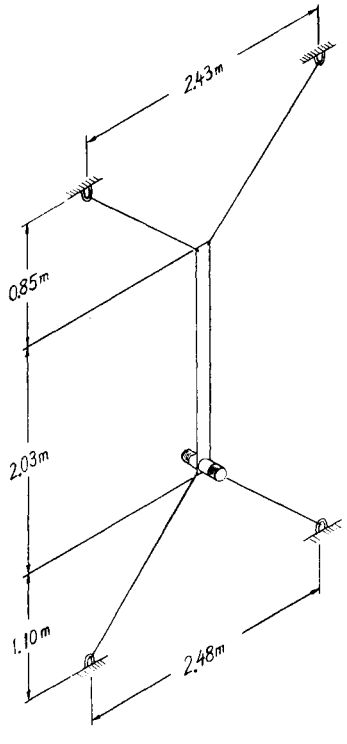


**Fig. 1 Beam-cable structure.**

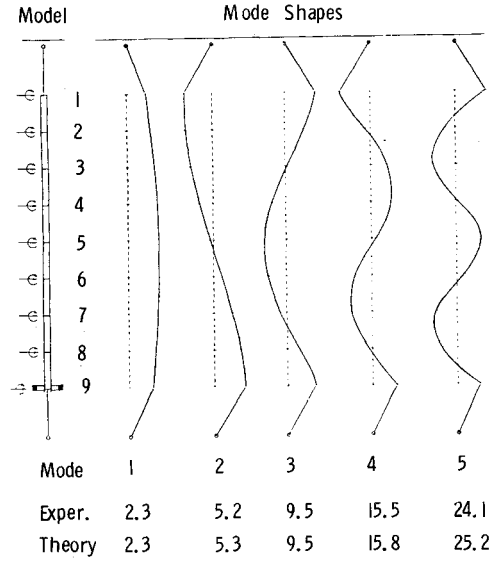


| | Mode | 1 | 2 | 3 | 4 | 5 |
|---|---|---|---|---|---|---|
| Freq. (Hz) | Exper. | 2.3 | 5.2 | 9.5 | 15.5 | 24.1 |
| | Theory | 2.3 | 5.3 | 9.5 | 15.8 | 25.2 |

**Fig. 2 Theoretical model (all DOFs shown, node numbers labeled), theoretical mode shapes, experimental and theoretical natural frequencies.**

**Table 1 Control strength sensitivity to added masses, $dc/dm_i$, $s^{-1}$**

| Lumped mass | Baseline design | Optimal design |
|---|---|---|
| 1 | −24.23 | −10.82 |
| 2 | 8.18 | 3.13 |
| 3 | −22.71 | −9.06 |
| 4 | 5.17 | 0.15 |
| 5 | 0.73 | 2.77 |
| 6 | −36.04 | −18.47 |
| 7 | 42.75 | 18.50 |
| 8 | −77.39 | −18.32 |
| 9 | 155.21 | 72.17 |

**Table 2 Control strength sensitivity to changes in element thickness, $dc/dh_i$, N-s/cm$^2$**

| Element | Baseline design | Optimal design |
|---|---|---|
| 1 | −0.1356 | −0.0630 |
| 2 | 0.0138 | −0.0251 |
| 3 | 0.2139 | 0.1517 |
| 4 | −0.2371 | −0.0987 |
| 5 | 0.3217 | 0.2340 |
| 6 | −0.2461 | −0.2392 |
| 7 | −0.2182 | −0.2062 |
| 8 | 0.6510 | 0.5934 |

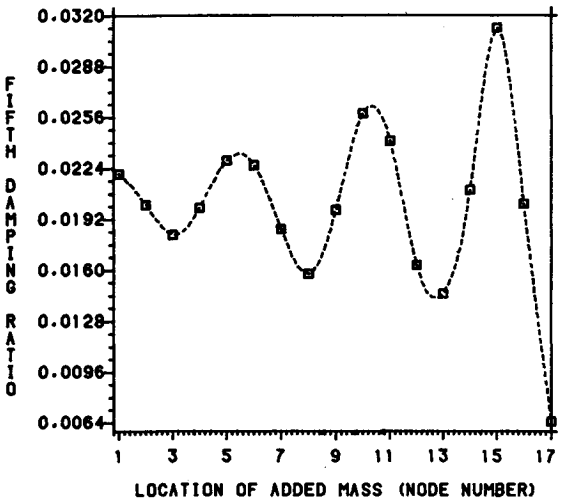


**Fig. 3 Fifth damping ratio $\zeta_5$ as a function of the position of 10% added mass for 16 finite element model, $c=0.1322$ (Ns/cm).**

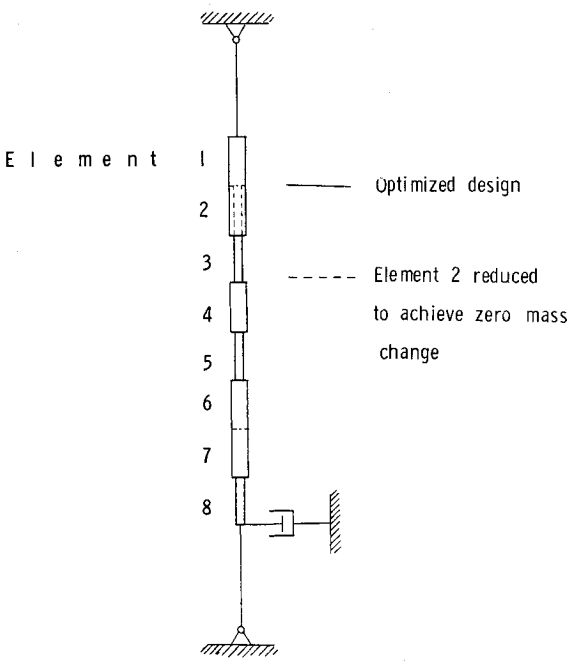


**Fig. 4 Optimal thickness distribution.**

fected by a rate feedback control involving a single force actuator colocated with a velocity sensor. The instantaneous control force is directly proportional, but opposite in sign, to the instantaneous velocity. This is equivalent to the attachment of a viscous dashpot to the structural DOF of the sensor, with the ratio of controlling force to sensed velocity being the viscous damping coefficient $c$. Therefore, $c$ is defined to be the measure of control strength. The control sensor and actuator are located at the bottom of the beam, as shown in Fig. 2 for an 8-element model.

Preliminary studies were done on three analytical models, with the beam modeled by 4, 8, and 16 equal finite elements, respectively. The results showed that the 8-element model was sufficiently accurate for further analysis.

## Results and Discussion

All results were obtained for the beam structure modeled by eight beam finite elements and having 18 DOF. The uniform-thickness beam without any additional masses is called the baseline design.

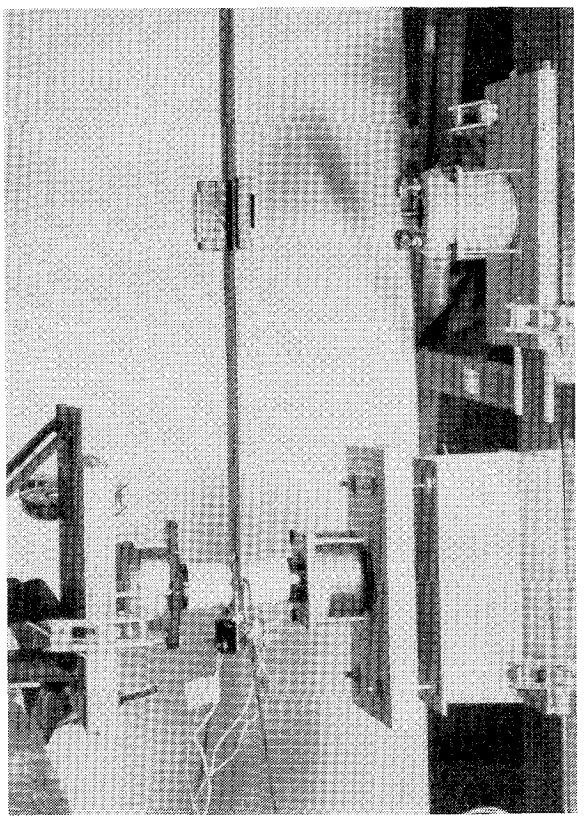

**Fig. 5 Lower portion of beam, including added mass, velocity sensor, and force actuator.**

**Table 3 Effect of design requirements on reduction in control strength afforded by 10% mass increase, constraints imposed on $\zeta_r$**

| Required lower limit on damping ratio | Control strength $c$, N-s/cm | | Reduction in control strength, % |
|---|---|---|---|
| | Baseline design | Design with 10% added mass | |
| 0.010 | 0.0658 | 0.0413 | 37.2 |
| 0.015 | 0.1002 | 0.0620 | 38.1 |
| 0.020 | 0.1364 | 0.0830 | 39.1 |
| 0.025 | 0.1756 | 0.1044 | 40.5 |
| 0.030 | 0.2204 | 0.1264 | 42.6 |

First, the control system was designed for the baseline design. The requirements imposed on the control system for the first five modes were $\zeta_r \geq 0.03$, $r=1,2,3,4,5$. This requirement was satisfied with $c=0.2204$ N-s/cm. For this value of $c$, $\zeta_5$ was equal to 0.03, and the first four damping ratios were above this value.

Next, the effect of adding small masses at the nine nodes of the finite element model was investigated. The sensitivity of the control strength $c$ with respect to the masses $dc/dm_i$ ($i=1$ through 9) was obtained for the baseline design for $\zeta_5$ constant (see Table 1). The results show that $dc/dm_8$ is the largest negative derivative and predict that the control requirement $c$ would be reduced by 88.5% relative to the baseline value by adding 10% of the baseline beam mass at node 8, which is 25.4 cm above the beam bottom (see Fig. 2).

Next, the optimization was performed with actual additional lumped masses at each of the nine beam nodes defined as the structure design variables. The total added mass was constrained not to exceed 10% of the baseline beam mass, and the same requirements were imposed on the control system as on the baseline design. The optimization concentrated the entire 10% added mass at node 8 and reduced the

required damping strength $c$ to 0.1264 N-s/cm, a 42.6% reduction relative to the baseline value. The only critical damping constraint was the lower limit on $\zeta_5$. The difference between the linear prediction of 88.5% reduction in $c$ and the actual value of 42.6% is due to the rapid changes in $dc/dm_i$ as mass is added. The values of $dc/dm_i$ for the final design are also given in Table 1 and show that the potential for further improvements in $c$ is much reduced.

The variation of the fifth eigenvalue decay rate $\zeta_5$ (the most critical constraint) was plotted as a function of the position of the added mass (see Fig. 3) for the beam modeled with 16 finite elements. It is clear from the figure why all the added mass is lumped at the single node and also that there are several local extrema.

The 42.6% reduction in required control strength by 10% mass addition is a clear synergistic effect. Because it requires an increase in total mass, however, it was considered to be less attractive than achieving a similar result by modifying the thicknesses of the beam finite elements. Such modification changes both stiffness and mass, and it permits the possibility of mass redistribution without any net growth. Therefore, the next design study was performed with the thickness of the beam elements $h_i$ being design variables, and constrained to vary no more than 10% from their original baseline value, 3.2 mm. The demands on the control system were the same as in the previous case.

First, the potential for improvement was assessed by calculating $dc/dh_i$ for the baseline design. The results in Table 2 show that the maximum derivative is for element 8 and that for this element a 10% decrease in thickness ($\Delta h = -0.32$ mm) is expected to reduce $c$ by 9.4%. Next, the optimization was performed resulting in a thickness distribution shown (by the solid lines) in Fig. 4, and the required damping strength $c$ was reduced to 0.1625 N-s/cm or by 26.3%, with a 2.5% increase in weight over the baseline design. Again, the constraint on the damping ratio of the fifth mode $\zeta_5$ was active, indicating, therefore, that the structure is controlled by controlling the fifth mode of vibration.

The sensitivity of control $c$ with respect to thickness ($dc/dh_i$ $i=1$ through 8) for the optimal design is also given in Table 2. The results showed in both cases that $dc/dh_2$ was small compared to the other sensitivity derivatives. Therefore, the thickness of the second element of the optimal design was reduced to its lower limit. This new design (shown by the broken line in Fig. 4) has no increase in mass relative to the baseline design, and it requires $c=0.1637$ N-s/cm or 25.7% less than baseline design.

Next, the effect of the design requirement on the damping was investigated for the 10% added mass design. The lower limit on modal damping ratio was varied from 0.010 to 0.030, and the same design procedure as above was applied.

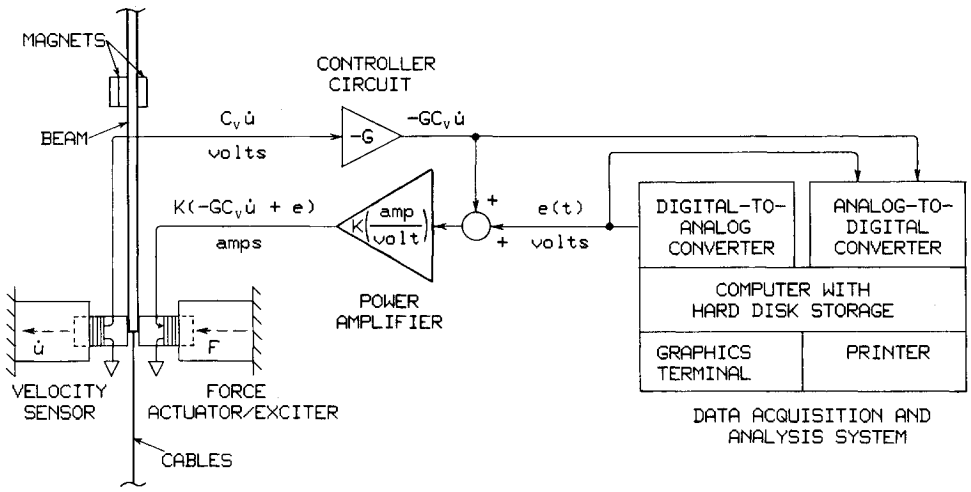


**Fig. 6 Schematic diagram of experimental apparatus.**

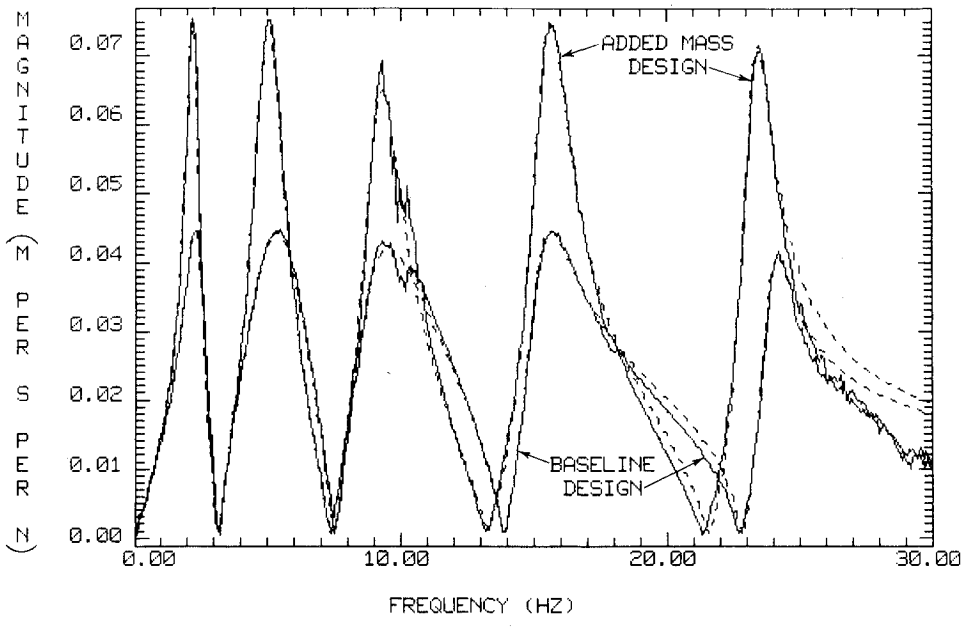


**Fig. 7 Experimental driving-point frequency response magnitudes for beam's bottom edge. Solid curves are experimental data; dashed curves are theoretical fits to the data.**

The results are shown in Table 3. In all cases, the optimization procedure lumped the total added mass 25.4 cm above the beam bottom (node 8), and the fifth mode damping ratio was the only active behavior constraint.

Instead of imposing constraints on damping ratios, i.e., on the number of cycles required for decay of vibration, one can alternatively impose constraints on the time $\tau_r$ of vibration decay by constraining the real parts of eigenvalues $\sigma_r$. Three designs obtained by imposing constraints on $\sigma_r$ are shown in Table 4. In all these designs the upper limit on $\sigma_1$ was the active constraint, which means that the first mode is controlling the design. These results indicate that small changes in design variables affect control gain very little and that the synergistic effect is nonexistent since the first mode, in which the beam essentially moves as a rigid body (see Fig. 2), is less sensitive to structural changes than the fifth one.

## Experimental Apparatus and Procedure

An experiment was conducted to determine how well the theory predicts reality. The cases tested in the experimental study were the baseline beam-cable design and the design that was optimized by means of an added mass for $\zeta_r \geq 0.03$. Frequency response functions were measured on the beam-cable laboratory structure, and values of $\zeta_r$ and $\omega_{0r}$ were inferred from the data for comparison with theoretical predictions.

The basic experimental apparatus and procedures have been described at length in Ref. 9. That description is summarized here, and some new aspects of apparatus and procedure relevant to this paper are described. Figure 5 is a photograph of the lower portion of the beam showing the mass added around node 8 and the control sensor and actuator.

The added mass consisted of several small magnets with collective weight equal to 10% of the weight of the beam. The magnets were held firmly to the steel beam by their own magnetic field. The added mass was distributed around, rather than concentrated at, node 8, and the distribution also added some rotational inertia to the beam. The consequences of the added mass being distributed rather than concentrated were considered to be negligible for the lowest five structural vibration modes, so the distribution was not included in the theoretical model. The small additional beam and cable tension produced by the weight of the magnets was also considered negligible and was not accounted for theoretically.

Figure 6 represents the structure and the control and instrumentation systems. The velocity sensor and force actuator consisted of structure-borne conducting coils interacting with concentrated, radial magnetic fields produced by stationary, noncontacting magnetic-field structures.[9]

The analog controller circuit indicated in Fig. 6 consisted of a few integrated circuit operational amplifiers and some resistors and a potentiometer to produce gain $G$.[9] In addition to producing the gain, the circuit served as a high impedance buffer, which helped to minimize current flow in the velocity-sensing coil.

The power amplifier indicated in Fig. 6 was designed to produce controlled current output rather than the more standard controlled voltage output.[10] This was necessary to establish a constant transduction of controller output voltage into actuator force, eliminating the effect of voltage induced by motion of the actuator coil. The transduction constant was calibrated as $K = 0.25$ A/V.

The data acquisition and analysis system indicated in Fig. 6 was developed by Synergistic Technology, Inc., of Cupertino, Calif. It provided excitation signal $e(t)$, as well as acquiring response and excitation signals and performing all data analysis. The excitation signal was added to the control feedback signal as input into the force-producing coil. Thus, that coil served the dual function of control actuator and exciter.

The relationship of the control system to the theoretical viscous damping constant $c$ can be developed with use of the notation given on Fig. 6. From elementary electromechanics theory,[9] the voltage generated by the velocity-sensing coil moving with velocity $\dot{u}$ is $C_v\dot{u}$, and the force generated by the force-producing coil carrying current $i$ is $C_f i$. $C_v$ and $C_f$ are constants (for $u$ within the linear range) measured on the apparatus of Fig. 5 to be 2.4 V/m/s and 2.4 N/A, respectively. Thus, from Fig. 6 the force generated is

$$F = C_f K(-GC_v\dot{u} + e) \tag{23}$$

Hence the viscous damping constant is

$$c = GKC_fC_v \tag{24}$$

With the desired value of $c$ given, control gain $G$ is calculated from this equation.

Velocity-to-force ($\dot{u}/F$) frequency response functions (FRF) were measured. Random excitation $e(t)$ was used. To achieve a good signal-to-noise ratio, the general excitation level was set as high as possible consistent with maintaining linear behavior of the velocity-sensing and force-producing coils. The linear range was approximately $|u| < 2$ mm. Fast Fourier transforms of the response and excitation signals were calculated, and the former was divided by the latter to produce an FRF. The frequency resolution was 0.0781 Hz. In all cases, the FRF calculated from a single excitation period without data windowing was reasonably smooth and reproducible, so neither averaging nor windowing were used. FRFs relating velocity output at node 9 to force input at node 8 were also measured (see the shaker in Fig. 5), but the data are not included in this paper.

## Experimental Results and Comparison with Theory

Representative FRF magnitudes are plotted on Fig. 7. The solid curves are the experimentally measured data for the baseline and 10%-added-mass designs, and the dashed curves are curve fits to the experimental data. The curve fitting was based on a five-mode theoretical model, and it was performed by the standard software of the data acquisition and analysis system. The curve fits are clearly very good. The only significant deviation is at frequencies above that of the fifth mode, and this had a negligible effect on the calculated values of modal damping and frequency. The high-frequency deviation was due to the absence of a sixth mode in the curve fit theoretical model.

The curve fit analysis calculated for each complex structural mode a damping ratio $\zeta_r$, a frequency $\omega_{0r}$, and a complex amplitude value. The former two are relevant to this study and are listed in Table 5, along with the theoretically predicted values.

Experimental and theoretical frequency values agree very well. The differences shown for mode 5 are probably due to the relatively low order of the structure finite element model, which gives an undamped natural frequency of mode 5 about 1 Hz too high.

**Table 4 Effect of design requirements on the reduction in control strength afforded by mass increase, constraints imposed on $\sigma_r$**

| Required upper limit on real part of eigenvalues, $s^{-1}$ | Time decay, s | Control strength $c$, N-s/cm: Baseline design | Control strength $c$, N-s/cm: Design with added mass | Reduction in control strength, % |
|---|---|---|---|---|
| −0.7175 | 1.39 | 0.0520 | 0.0510 | 1.9 |
| −1.4350 | 0.69 | 0.1033 | 0.1010 | 2.2 |
| −2.1525 | 0.46 | 0.1532 | 0.1492 | 2.6 |

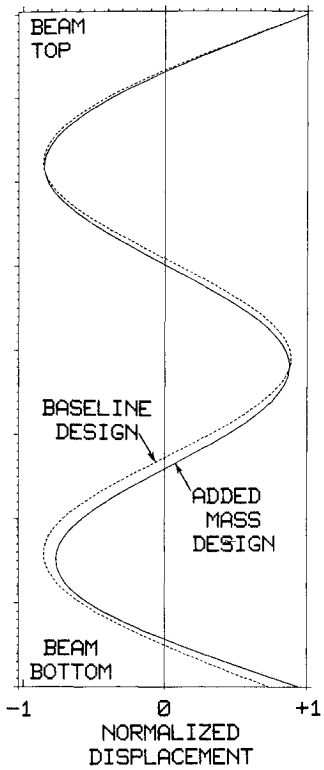


**Fig. 8 Calculated fifth mode shape of the beam.**

**Table 5 Experimental and theoretical damping and frequency values**

| Structural vibration mode $r$ | $\zeta_r$ | | $\omega_{0r}/2\pi$, Hz | |
|---|---|---|---|---|
| | Experiment | Theory | Experiment | Theory |
| | Baseline design | | | |
| 1 | 0.177 | 0.200 | 2.5 | 2.5 |
| 2 | 0.270 | 0.314 | 5.6 | 5.5 |
| 3 | 0.169 | 0.156 | 8.9 | 8.8 |
| 4 | 0.061 | 0.064 | 15.2 | 15.3 |
| 5 | 0.025 | 0.030 | 23.9 | 24.9 |
| | 10% added mass design | | | |
| 1 | 0.116 | 0.125 | 2.2 | 2.2 |
| 2 | 0.116 | 0.121 | 5.1 | 5.0 |
| 3 | 0.080 | 0.071 | 9.2 | 9.3 |
| 4 | 0.046 | 0.049 | 15.5 | 15.6 |
| 5 | 0.025 | 0.030 | 23.4 | 24.2 |

There is good quantitative agreement between experimental and theoretical damping ratios. The differences may be explained in part by the omission of inherent passive damping from the theoretical model. Inherent damping of the lightly damped beam-cable structure has proved difficult to measure accurately. It has been determined, however, that the inherent damping ratios are on the order of 0.001 for modes 1 and 2 (cable deformation modes in which the beam moves primarily as a rigid body), 0.01 for mode 3 (free-free beam first bending mode), and 0.005 for modes 4 and 5 (free-free beam higher bending modes). The higher inherent damping in mode 3 may explain why this is the only mode, for both designs, for which experimental damping exceeds theoretical damping.

Comparison of theoretical and experimental damping values suggests strongly that the control system produced a damping constant $c$ which was lower than expected, or that some calibration factor or factors were incorrect. However, several independent checks of both the control system and the data acquisition system failed to confirm these suspicions. So the small but consistent discrepancies in damping values remain unexplained.

The investigation of these discrepancies produced one significant observation. Formerly, the centerline of the sensor-actuator pair of coils was positioned about 1 cm above the beam's bottom edge (node 9), and the value of $\zeta_5$ measured for both designs was about 0.020. But the vicinity of the bottom edge is a region of very steep gradient in the normal mode shape of the fifth undamped structure mode, as shown in Fig. 8. So this positioning error was important relative to the active damping provided to that mode. Repositioning the centerline of the coils downward by only 1 cm produced the 25% increase in $\zeta_5$ shown in Table 5.

The reader might note in Fig. 7 the significant difference in fifth mode peak magnitude between the baseline and added mass designs, even though both have the same value of $\zeta_5$. This is explained by Fig. 8, which shows that the added mass design has substantially greater modal displacement at the beam's bottom edge than does the baseline design.

## Concluding Remarks

A procedure for checking whether small changes in a structure have the potential for significant enhancements of its vibration control system was developed. The first step in the procedure consists of the calculation of the sensitivity of the required strength of the control system to small changes in structural parameters. The second step consists of the optimization of the structural parameters to produce maximal reduction in required control system strength with minimal change in the structure.

A flexible beam structure supported by four cables and controlled by a rate feedback, single-colocated, force-actuator velocity-sensor pair was used to demonstrate the procedure. Analytical calculations predicted that substantial reduction in control strength requirement can be achieved with minimal changes in the structure. These theoretical predictions were validated experimentally with good agreement between theory and test.

## Acknowledgments

The research reported in this paper was supported in part by NASA Grant NAG-1-224. The experimental equipment was purchased with the aid of NSF Grant CME-8014059. The help of Mr. George Schamel in running the experiments and preparing the manuscript is gratefully acknowledged.

## References

[1]NASA Scientific and Technical Information Branch, "Technology for Large Space Systems—A Bibliography with Index," NASA SP-7046(09), July 1983.

[2]Skelton, R. E. and DeLorenzo, M. L., "Selection of Noisy Actuators and Sensors in Linear Stochastic Systems," *Journal of Large Scale Systems, Theory and Applications*, Vol. 4, 1983, pp. 109-136.

[3]Lindberg, R. E. and Longman, R. W., "On the Number and Placement of Actuators for Independent Modal Space Control," *Journal of Guidance, Control and Dynamics*, Vol. 7, March-April 1984, pp. 215-221.

[4]Horner, G. C., "Optimum Actuator Placement, Gain and Number for a Two-Dimensional Grillage," AIAA Paper 83-0854, May 1983.

[5]Hale, A. L. and Lisowsky, R. J., "Optimal Simultaneous Structural and Control Design of Maneuvering Flexible Spacecraft," presented at the Fourth VPI & SU/AIAA Symposium on Dynamics and Control of Large Structures, June 6-8, 1983.

[6]Haftka, R. T., "Design for Temperature and Thermal Buckling Constraints Employing a Non-Eigenvalue Formulation," *Journal of Spacecraft and Rockets*, Vol. 20, July-Aug. 1983, pp. 363-367.

[7]Rogers, L. C., "Derivatives of Eigenvalues and Eigenvectors," *AIAA Journal*, Vol. 8, May 1970, pp. 943-944.

[8]Miura, H. and Schmit, L. A., "NEWSUMT—A Fortran Program for Inequality Constrained Function Minimization—Users Guide," NASA CR 159070, June 1979.

[9]Hallauer, W. L. Jr., Skidmore, G. R., and Mesquita, L. C., "Experimental-Theoretical Study of Active Vibration Control," *Proceedings of the 1st International Modal Analysis Conference*, Union College, Schenectady, N.Y., 1982, pp. 39-45.

[10]Skidmore, G. R., "A Study of Modal-Space Control of a Beam-Cable Structure: Experiment and Theory," M.S. Thesis, Virginia Polytechnic Institute and State University, Blacksburg, Va., 1983.